Electronics and Electrical Engineering

AIMS Electronics and Electrical Engineering, 6(4): 385–396.
DOI: 10.3934/electreng.2022023
Received: 26 April 2022
Revised: 08 August 2022
Accepted: 17 August 2022
Published: 08 October 2022

http://www.aimspress.com/journal/ElectrEng

Research article

Design of electromagnetic cloak with sequentially connected rectangular split ring resonators for S-band applications

Srilatha K[1], B T P Madhav[1,*], Krishna J[1], Y V N R Swamy Banothu[2] and Anil Badisa[3]

[1] Antennas and Liquid Crystals Research Centre, Department of ECE, Koneru Lakshmaiah Education Foundation, Andhra Pradesh, India
[2] ECE Department, Lakireddy Bali Reddy College of Engineering (Autonomous), Mylavaram, India
[3] Department of ECE, GMR Institute of Technology, Rajam, Andhra Pradesh, India

* **Correspondence:** Email: btpmadhav@kluniversity.in.

Abstract: An electromagnetic (EM) invisible cloak is designed and analyzed with serially interconnected split ring resonators (SRRs). The cloak consists of an array of a network of split ring resonators which operates at a 3 GHz resonating frequency. The split ring resonators are connected with transmission line and are wrapped around the cylindrical object. Cloak coupled with EM waves gets transferred around the cylindrical object and received to the other side of transmission. Scattering cross section (SCS) is analyzed for both cases, which results in the effect of resonance. The total scattering cross section of the cloaked object is reduced by using SRRs. The simulated and measured results are in great agreement with each other. The transmission-line-connected SRR cloak is useful for S-band applications specifically at 3 GHz resonance.

Keywords: split ring resonators (SRR); scattering cross section (SCS); EM waves; cloaked object

1. Introduction

Cloaking has acquired immense attention from researchers and scientists in every aspect because of its electromagnetic behavior. Cloaking can be achieved in different ways: the transmission line approach, the mantle cloak approach, the transformation optics approach and surface wave cloaks. There are some other techniques used for cloaking, like plasmonic resonance and the scattering cancellation technique with polarization dependent angle of incidence [1–3]. All these techniques are used to achieve cloaking towards electromagnetic waves. Cloaking is used in invisible sensors in medical applications like non-invasive detections, energy harvesters [4], etc. Though the cloaks are used in many applications, there are some limitations like narrow band operation and single band operation [5–8]. To overcome these drawbacks, surface wave cloaks are used where a gradient index material is used as a dielectric substrate to achieve cloaking. Multiband cloaks are also available which are applicable for many applications and have more flexibility of cloaking, offering multiple bands. Multilayer cloaking is used to achieve multiband cloaking. Multiple layers of structures are used, and this leads to increased cloak size [9–12].

Some research work has been done with the usage of LC based circuits which can act as metamaterials. A microwave network-based concept has been used where multiple patches are used to achieve multiband operation. In this case, the size of the cloak is small, and operating frequencies are under control [13,14]. The cloak with patches is also used for multiple operational bands, where the vertical length of the array increases the frequency ratio [15–18]. The nonmagnetic metamaterial cloaks are also designed with the usage of split ring resonators, which suits for optical cloaking with the formation of a greater number of layers around the cylindrical object, which leads to an increase in the size of the device [19,20]. The permeability of the spilt ring resonator plays a key role in cloaking the object [21]. The transmission line cloak, with a greater number of layers, is considered to reduce the total scattering cross section (SCS) of the cloaked object [22]. The split ring resonator, which acts as a metamaterial cell, is useful for many applications, like in antennas implemented with neural networks, etc. [23,24]. The main aim of this work is to cloak an object with split ring resonators interconnected with each other to replace the microstrip interconnected patches. The selection of a compact array size leads to good cloaking effects with reduced reflections.

This work explains the replacement of patches with a Split Ring Resonator (SRRs) based network with sequentially interconnected SRRs. The microstrip patches are replaced with SRRs. The split ring resonators achieve good cloaking effect as compared with the microstrip patches. The SRRs have the capability to modify the resonant frequency by altering the unit cell size. The unit cell is designed as a rectangular SRR with transmission line connected on both sides of the SRR. The unit cell is developed as an array and wrapped over the cylindrical dielectric object with a radius of 30 mm. The SRR structure exhibits metamaterial properties, and by making significant changes in the material structure, one can achieve effective resonance at wavelengths much larger than the diameter of the ring. The SRRs are interconnected with the transmission line and arranged to achieve the desirable cloaking effect at 3 GHz resonating frequency.

2. Unit cell design and its analysis

A rectangular split ring resonator is designed instead of a patch model for cloaking. The design has transmission lines on both sides of split ring resonators. Copper is used as the conducting element for the front side, and a full ground copper patch is used for the back side of the unit cell structure. The dielectric substrate used is Rogers RO3010 with a dielectric constant of $\varepsilon_r = 10.2$ and a loss tangent of 1.6, along with 0.035 mm of copper thickness. The simulation part is totally done using CST. The boundaries in the x and y directions are each set to be an "Open Boundary," while the upper boundary in the z direction is set to be an "Open Add Space Boundary" so that Port 3 keeps a distance from the cloak unit cell. The front view and back view of the proposed unit cell is shown in Figure 1, with its dimensional parameters listed in Table 1.

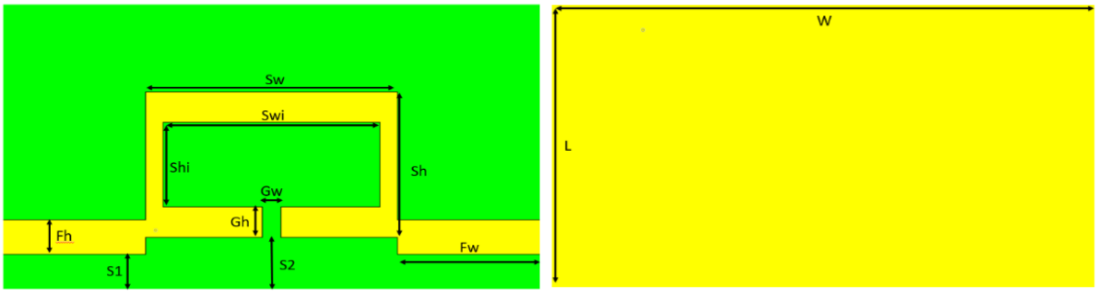

Figure 1. Front view and back view of the proposed unit cell with parameters (given in Table 1).

Table 1. Dimensional parameters of the proposed unit cell.

Parameter	Value (in mm)
L	16
W	28.12
Fh	1.92
Fw	7.5
S1	2
S2	2.96
Sw	13.12
Sh	8.08
Swi	12.28
Shi	4.72
Gw	0.96
Gh	1.68

The analysis of the unit cell is carried out with three wave ports. Two wave ports are placed on either side of the transmission line, and the third port is applied on the top of the unit cell where electromagnetic waves are incident on the structure. The design of the proposed unit cell with proper wave ports is shown in Figure 2. The SRR is adjusted with respect to the transmission line to acquire the desired results with reduced reflections. At the first step (iteration), the SRR is connected to transmission line, which results in huge reflections. So, in order to reduce the reflections, the SRR is adjusted by half the width of the transmission line. Open boundaries are applied along the x and y directions, whereas an open add space boundary is given in the z direction.

The proposed unit cell satisfies a few conditions [14] to work as a cloak, which are $S_{11} -> 0, S_{21} -> 1$ $S_{33} -> 0$ and $S_{3(1+2)} -> 1$. These are the primary conditions needed to work as a cloak. The transmission and reflection coefficients are represented as S_{21}/ S_{12} and S_{11}/ S_{22} of port 1 and port 2. S_{33} is given as the coupling of incident waves into the patch, and $S_{3(1+2)}$ represents the coupling of waves back into space. The S-parameter values obtained for the designed unit cell with 3 GHz resonant frequency are S_{11} = -39.7 dB, S_{21} = -0.7 dB, S_{33} = -9.5 dB, S_{31} =-36.6 dB and S_{32} = -36.8 dB.

The S_{31} and S_{32} values obtained seem to be less than S_{11} but close to it. Even though the values are close, cloaking can be obtained. So, by considering this point, we can assume the values of S_{31} and S_{32} can be less than S_{11} to achieve cloaking. Figure 3 shows the scattering parameters of the unit cell. S_{33} obtained is less than -10 dB which is also need to be an important parameter for resonance.

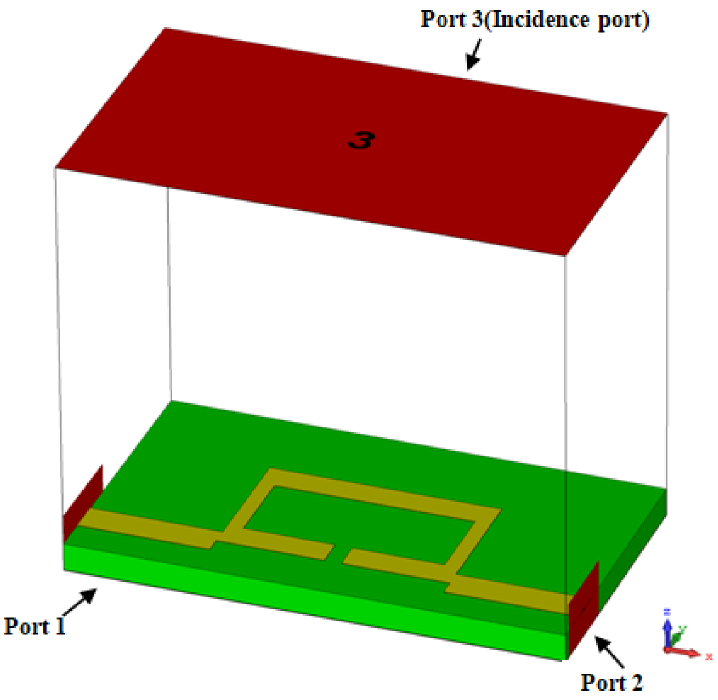

Figure 2. Simulated geometry of the proposed unit cell with wave ports.

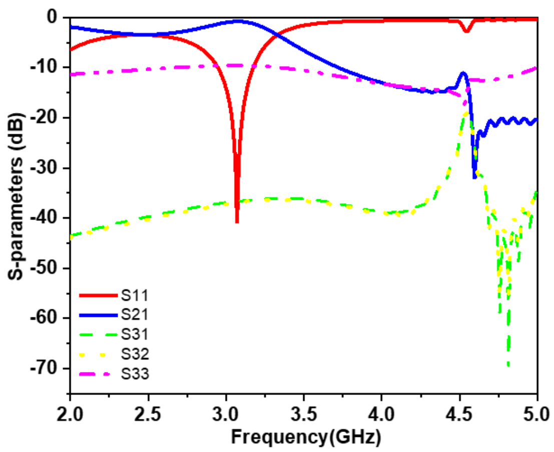

Figure 3. Simulated scattering parameters of the proposed unit cell.

All the S-parameters are analyzed by simulating the unit cell with three-port analysis. The results reveal that the condition that needs to be satisfied for cloaking with 3-port analysis is that the S_{31}, S_{32} and S_{33} values are less than S_{11}. If this condition is satisfied, then the structure is said to be exhibiting cloaking characteristics. However, when observing Figure 3, the results obtained suits for only lower frequencies.

3. Design of cloak with proposed unit cell

A cylinder is taken into consideration, having a radius of 30 mm with a height of 16 mm. Seven-unit cells are connected to each other to cover the designed cylindrical object, acting as a cloak. A single row is designed, i.e., a 1 x 7 sized array is taken into consideration. The dielectric substrate is wrapped over the cylinder by using the "cylindrical bend" option in the CST Microwave Studio. Then, the 1 x 7 array is wrapped over the substrate, which acts as a cloak. The simulated cylindrical cloak and its fabricated model are shown in Figure 4.

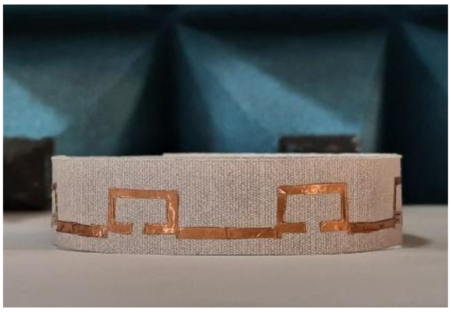

Figure 4. Proposed cylindrical cloak: (a) Simulated geometry with x-axis incidence, (b) Fabricated cloak.

The number of patches (*n*) required to wrap a single layer of the cylinder is calculated below using Equation 1. Effective relative permittivity is calculated by Equation 2. Effective length of the feedline to be adjusted to wrap the entire cylinder is calculated by Equation 3.

The mathematical representations of the cloak to wrap over the cylinder are given below [13]:

$$n = \frac{2\Pi(r+h) - \frac{4r}{\sqrt{\varepsilon_{reff}}}}{Sw} \tag{1}$$

$$\varepsilon_{reff} = \frac{\varepsilon_r+1}{2} + \frac{\varepsilon_{r-1}}{2}\left\{\left(1+12\frac{h}{Fh}\right)^{-1} + 0.04\left(1-\frac{Fh}{h}\right)^2\right\} \tag{2}$$

$$2 * Fw = \frac{2\Pi(r+h)}{n} - Sw \tag{3}$$

where
n is the number of patches required to wrap around a single cylindrical layer,
h is the thickness,
r is the radius of the cylinder,
ε_{reff} is the effective dielectric constant,
F_h is the width of the feedline,
Sw is the length of the patch,
Fw is the length of the feedline.

The conditions need to be justified to verify cloaking operation is as follows [6]:

- An infinitely long cylinder has to be considered with boundary conditions and are simulated, to calculate the reflection and transmission coefficients with and without the cloak.
- The magnitude and phase are analyzed through animated fields with respect to frequencies for both cases, with and without the cloak.
- Through S-parameters, the scattering cross section (SCS) and bistatic scattering width of the cylinder are calculated for the cases with and without the cloak.

To analyze all these conditions and to justify these characteristics, CST Microwave Studio is used with time domain solver along with proper boundary conditions [6]. The boundary conditions and background values are listed in Table 2.

Table 2. Boundary conditions and background values used to simulate the cloak.

Axis	Boundary condition	Background (in mm)
X	Open	200
Y	Open	50
Z	PEC	0

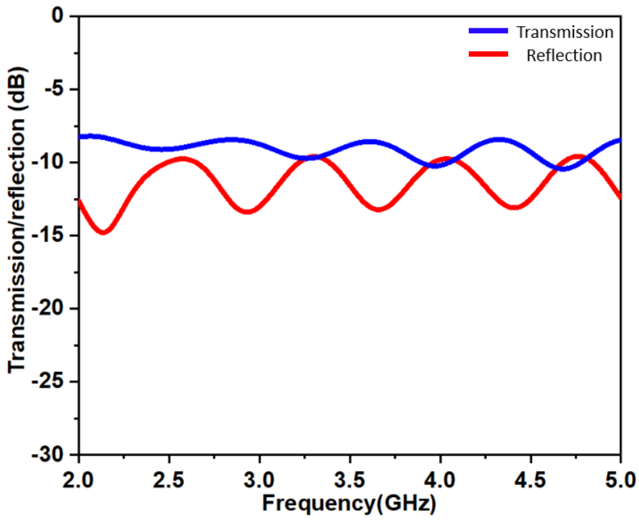

Figure 5. Simulated reflection (red) and transmission (blue) coefficients of a cylinder without cloak.

Figure 5 shows the reflection and transmission coefficients of a cylinder without cloak. There are no sharply resonant reflection and transmission features for the cylinder without cloak. Figure 6 shows the reflection and transmission for the cylinder with cloak. It is observed that the cloak resonates at 3 GHz frequency.

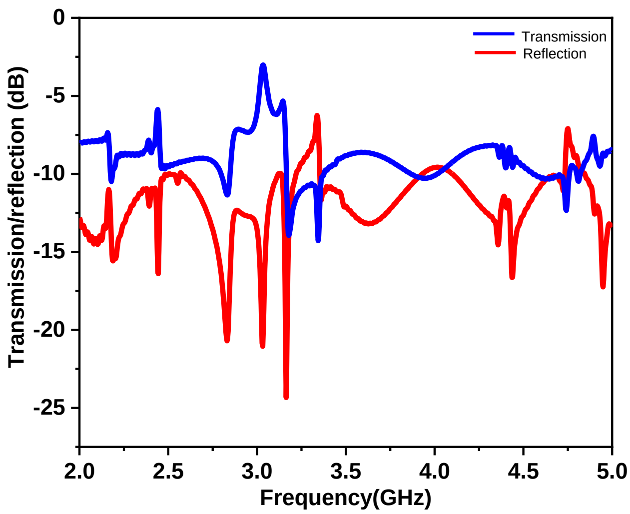

Figure 6. Simulated reflection and transmission coefficients of the cylinder with cloak.

There are some other possible reflections obtained, as we observe from Figure 6, but they are not quite desirable for transmission. Only at 3 GHz frequency does the structure operate as a cloak with satisfactory results in terms of reflection and transmission. Figure 7 shows the electric field distributions of the cloaked and bare cylinders. The fields in Figure 7(b) get diverted to other directions and cause high reflections. Figure 7(a) shows that the electric field in the case of the cloaked cylinder has lower deviations than in the case without the cloak.

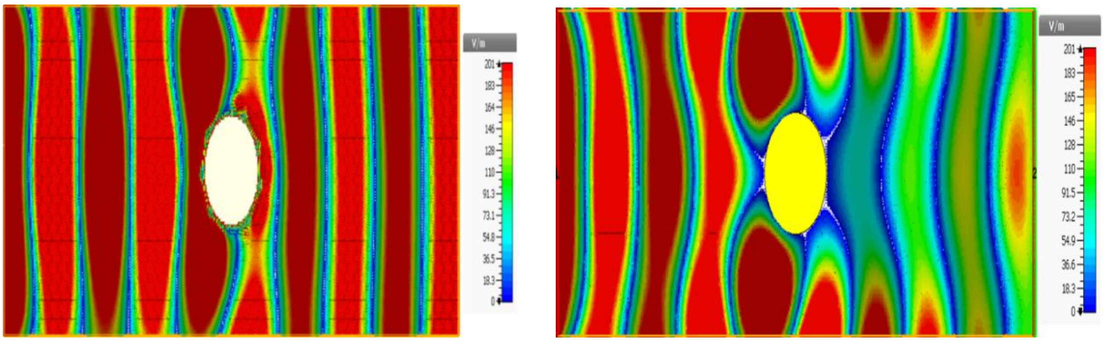

(a) (b)

Figure 7. Simulated electric field distributions of the cylinder at 3.03 GHz (a) with cloak and (b) without cloak.

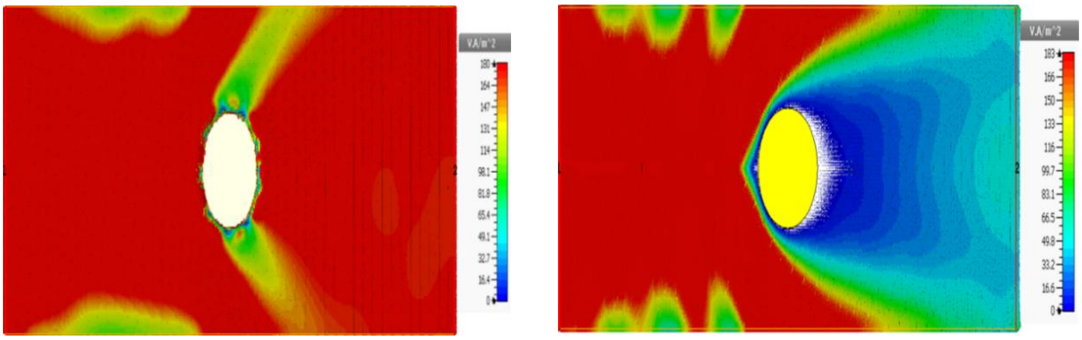

(a) (b)

Figure 8. Simulated power flow distributions of the cylinder at 3.03 GHz (a) with cloak and (b) without cloak.

Figure 8 shows the power flow distribution of the cylindrical object with and without cloak. The cloaking takes place in Figure 8(a), and the power flow is transferred the incident area to receiving side, by observing the circumference of the cylinder. Figure 8(b) shows that there is no transfer of the energy from the incident plane to the reception side of the cylinder.

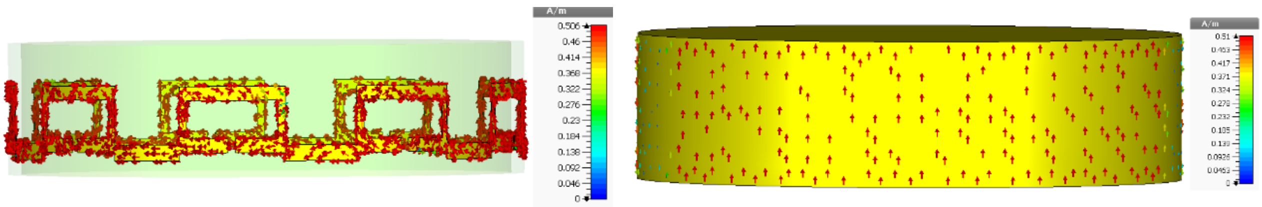

Figure 9. Simulated surface current distributions of the cylindrical object (a) with cloak and (b) without cloak.

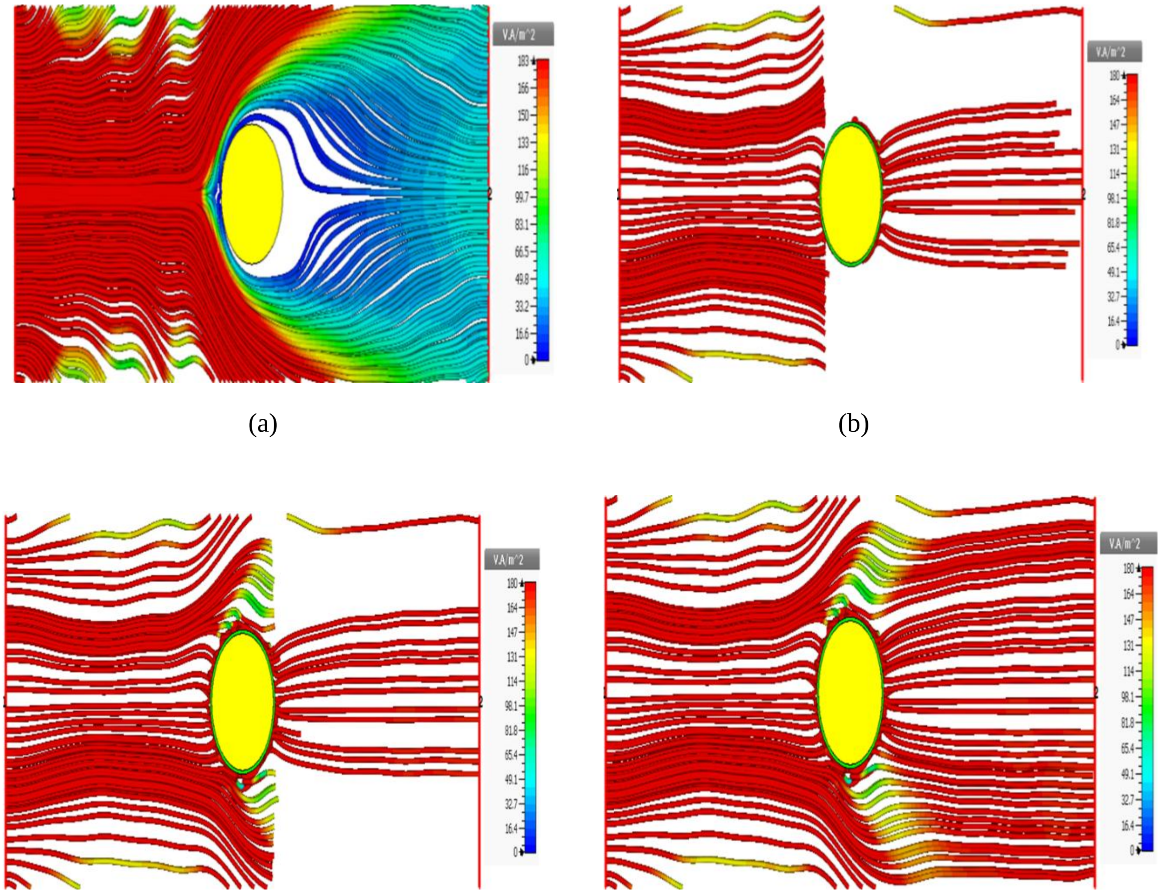

(a) (b)

(c) (d)

Figure 10. Simulated power flow distributions of the cylindrical object. Animated view screenshots at different instants (a) without cloak and (b, c, d) with cloak at 3.03 GHz resonant frequency.

Figure 9 shows the surface current distributions of the cylindrical object with and without cloak. The cloaked cylinder shows that the current distributions occur along the surface of the transmission-line-connected SRR patch, as shown in Figure 9(a). However, in the case of the uncloaked cylinder, as shown in Figure 9(b), the current is distributed all over the surface of the cylinder, indicating that no cloaking has been performed. Figure 10 shows the power flow of the cylindrical object without cloak in Figure 10(a) and with cloak at various instants from animated view in Figure 10(b, c, d). The field is disturbed around the uncloaked cylinder and gets diverted, as we observe from Figure 10(a), whereas the maximum power is transferred from the source to the destination for the cloaked cylinder, as shown in Figure 10(b, c, d).

Figure 11 shows the parametric analysis of a cloaked cylinder with a change of swi parameter of the designed unit cell in terms of $SCS_{t,\ norm}$. $SCS_{t,norm}$ depicts the behavior of normalized total scattering cross section of the cloaked cylinder. In CST Microwave Studio, with the application of some result templates, the scattering cross section is obtained with respect to frequency. The $SCS_{t,\ norm}$ shows that, for different swi parameter values, achieves lower SCS value with more change in frequency.

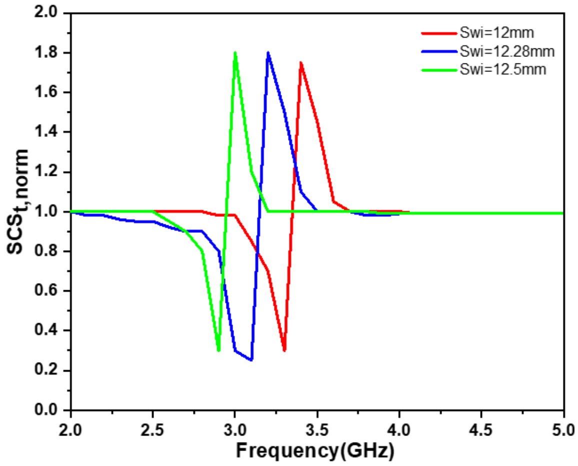

Figure 11. Simulated parametric analysis of $SCS_{t,\ norm}$ as a function of frequency for "swi."

The frequency variations obtained are small where SCS shifts to a high value. Figure 12 shows the $SCS_{t,\ norm}$ of cylinders with and without cloak. In the absence of cloak, the value is constant at one; and when the object gets cloaked, then SCS alters and is lower at 3 GHz frequency.

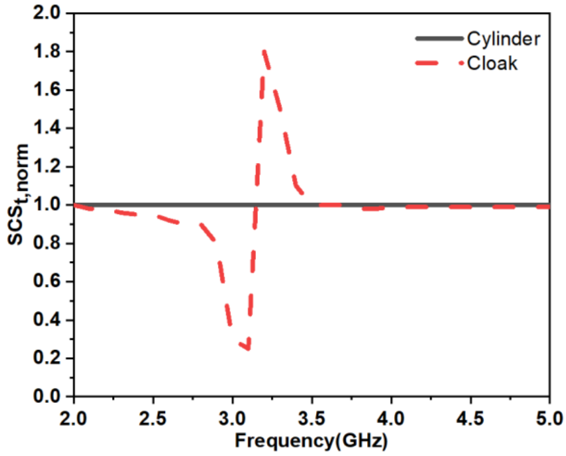

Figure 12. Simulated $SCS_{t,\ norm}$ of the object with and without cloak at 3 GHz resonant frequency.

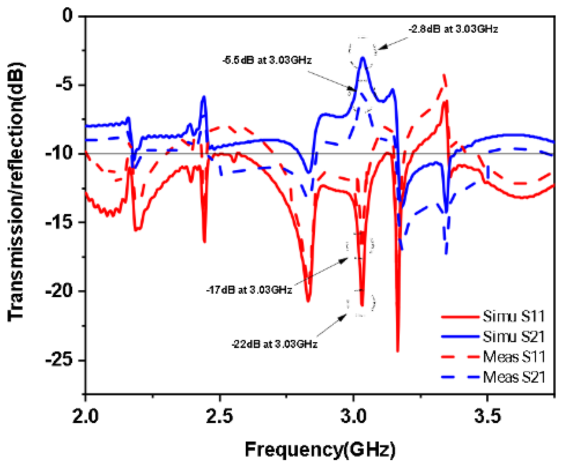

Figure 13. Comparison of simulated and measured S-parameter coefficients of cylindrical cloak.

Figure 13 shows the simulated and measured transmission and reflection coefficients of the cylindrical cloak. From Figure 13, we observe that the measured results show quite higher reflections as compared with simulated ones. However, the difference obtained is quite good for cloaking to operate at the required resonating frequency.

4. Conclusions

The sequentially connected split ring resonator based cylindrical cloak was proposed. The main aim of this work is to replace the patches with split ring resonators for cloaking applications. The proposed design is simulated and measured through S-parameters. Unit cell simulation is also done by using 3-port analysis. The array is designed with proper size to wrap over the cylinder to act as a cloak. The reflection and transmission coefficients, electric field distributions and power flow distributions are demonstrated for the cylindrical object with and without cloak. The designed cloak is operated at a 3 GHz resonant frequency with quite well pronounced cloaking effects. Finally, the scattering cross section with the proposed electromagnetic cloaking is reduced, and the interference also reduces to acceptable value.

Acknowledgments

We would like to thank DST through FIST support to the ECE department of KLEF (SR/FST/ET-II/2019/450).

Conflict of interest

The authors declare that they have no conflict of interest regarding this paper.

References

1. Nicorovici NAP, McPhedran RC (2008) Stefan Enoch, and Gérard Tayeb. "Finite wavelength cloaking by plasmonic resonance. *New J Phys* 10: 115020. https://doi.org/10.1088/1367-2630/10/11/115020
2. Silveirinha MG, Andrea A, Nader E (2008) Infrared and optical invisibility cloak with plasmonic implants based on scattering cancellation. *Phys Rev B* 78:: 075107. https://doi.org/10.1103/PhysRevB.78.075107
3. Serebryannikov AE, Alici KB, Ozbay E, et al. (2018) Thermally sensitive scattering of terahertz waves by coated cylinders for tunable invisibility and masking. *Opt Express* 26: 1–14. https://doi.org/10.1364/OE.26.000001
4. Alkurt FO, Altintas O, Ozakturk M, et al. (2020) Enhancement of image quality by using metamaterial inspired energy harvester. *Phys Lett A* 384: 126041. https://doi.org/10.1016/j.physleta.2019.126041
5. Schurig D, Mock JJ, Justice BJ, et al. (2006) Metamaterial electromagnetic cloak at microwave frequencies. *Science* 314: 977–980. https://doi.org/10.1126/science.1133628
6. Vehmas J, Alitalo P and Tretyakov SA (2011) Transmission-line cloak as an antenna. *IEEE Antenn Wirel Pr* 10: 1594–1597. https://doi.org/10.1109/LAWP.2011.2179000

7. Alitalo P, Culhaoglu AE, Osipov AV, et al. (2012) Experimental characterization of a broadband transmission-line cloak in free space. *IEEE T Antenn Propag* 60: 4963–4968. https://doi.org/10.1109/TAP.2012.2207339
8. Rajput A and Srivastava KV (2016) Approximated complementary cloak with diagonally homogeneous material parameters using shifted parabolic coordinate system. *IEEE T Antenn Propag* 65: 1458–1463. https://doi.org/10.1109/TAP.2016.2639015
9. Rajput A and Srivastava KV (2017) Dual-band cloak using microstrip patch with embedded u-shaped slot. *IEEE Antenn Wirel Pr* 16: 2848–2851. https://doi.org/10.1109/LAWP.2017.2749507
10. La Spada L, McManus TM, Dyke A, et al. (2016) Surface wave cloak from graded refractive index nanocomposites. *Scientific Reports* 6: 1–8. https://doi.org/10.1038/srep29363
11. McManus TM, La Spada L and Hao Y (2016) Isotropic and anisotropic surface wave cloaking techniques. *J Optics* 18: 044005. https://doi.org/10.1088/2040-8978/18/4/044005
12. Soric JC, Monti A, Toscano A, et al. (2015) Multiband and wideband bilayer mantle cloaks. *IEEE T Antenn Propag* 63: 3235–3240. https://doi.org/10.1109/TAP.2015.2421951
13. Rao PH, Balakrishna I and Sherlin BJ (2018) Radiation Blockage Reduction in Antennas Using Radio-Frequency Cloaks. *IEEE Antenn Propag M* 60: 91–100. https://doi.org/10.1109/MAP.2018.2818000
14. Wang J, Qu S, Xu Z, et al. (2012) Super-thin cloaks based on microwave networks. *IEEE T Antenn Propag* 61: 748–754. https://doi.org/10.1109/TAP.2012.2220326
15. Alù A and Engheta N (2008) Multifrequency optical invisibility cloak with layered plasmonic shells. *Phys rev lett* 100: 113901. https://doi.org/10.1103/PhysRevLett.100.113901
16. Shao J, Zhang H, Lin Y, et al. (2011) Dual-frequency electromagnetic cloaks enabled by LC-based metamaterial circuits. *Prog Electrom Res* 119: 225–237. https://doi.org/10.2528/PIER11052507
17. Wang J, Qu S, Xu Z, et al. (2014) Multifrequency super-thin cloaks. *Photonics Nanostruct* 12: 130–137. https://doi.org/10.1016/j.photonics.2013.11.003
18. Yan TC, Chen ZN and Hee D (2019) Single-layer dual-band microwave metasurface cloak of conducting cylinder. *IEEE T Antenn Propag* 67: 4286–4290. https://doi.org/10.1109/TAP.2019.2906504
19. Kanté B, Germain D and de Lustrac A (2009) Experimental demonstration of a nonmagnetic metamaterial cloak at microwave frequencies. *Phys Rev B* 80: 201104. https://doi.org/10.1103/PhysRevB.80.201104
20. Moghbeli E, Askari HR and Forouzeshfard MR (2018) The effect of geometric parameters of a single-gap SRR metamaterial on its electromagnetic properties as a unit cell of interior invisibility cloak in the microwave regime. *Opt Laser Technol* 108: 626–633. https://doi.org/10.1016/j.optlastec.2018.07.025
21. Moghbeli E, Askari HR and Forouzeshfard MR (2018) Analyzing the effect of geometric parameters of double split ring resonator on the effective permeability and designing a cloak of invisibility in microwave regime. *Applied Physics A* 124: 1–9. https://doi.org/10.1007/s00339-018-1774-3
22. Alitalo P and TretyakovS (2008) Cylindrical transmission-line cloak for microwave frequencies. *2008 International Workshop on Antenna Technology: Small Antennas and Novel Metamaterials*, 147–150. IEEE. https://doi.org/10.1109/IWAT.2008.4511309

23. Abdulkarim Y, Deng L, Yang J, et al. (2020) Tunable left-hand characteristics in multi-nested square-split-ring enabled metamaterials. *J Cent South Univ* 27: 1235–1246. https://doi.org/10.1007/s11771-020-4363-5
24. Sagik M, Karaaslan M, Ünal E, et al. (2021) C-shaped split ring resonator type metamaterial antenna design using neural network. *Opt Eng* 60: 047106. https://doi.org/10.1117/1.OE.60.4.047106